V.A.1 Fuel Cell Systems Analysis

Rajesh K. Ahluwalia (Primary Contact), Xiaohua Wang, Romesh Kumar
Argonne National Laboratory
9700 South Cass Avenue
Argonne, IL 60439
Phone: (630) 252-5979; Fax: (630) 252-5287
E-mail: walia@anl.gov

DOE Technology Development Manager: Jason Marcinkoski
Phone: (202) 586-7466; Fax: (202) 586-9811
E-mail: Jason.Marcinkoski@ee.doe.gov

Project Start Date: October 1, 2003
Project End Date: Project continuation and direction determined annually by DOE

Objectives

- Develop a validated model for automotive fuel cell systems (FCSs) and periodically update it to assess the status of technology.
- Conduct studies to improve performance and packaging, to reduce cost, and to identify key research and development issues.
- Compare and assess alternative configurations and systems for transportation and stationary applications.
- Support DOE/FreedomCAR automotive fuel cell development efforts.

Technical Barriers

This project addresses the following technical barriers from the Fuel Cells section of the Hydrogen, Fuel Cells and Infrastructure Technologies Program Multi-Year Research, Development and Demonstration Plan:

(B) Cost
(C) Performance
(E) System Thermal and Water Management
(F) Air Management
(J) Startup and Shutdown Time and Energy/Transient Operation

Technical Targets

This project is conducting system level analyses to address the following DOE 2010 technical targets for automotive fuel cell power systems operating on direct hydrogen:

- Energy efficiency: 50%-60% (55%-65% for stack) at 100%-25% of rated power
- Power density: 650 W/L for system, 2,000 W/L for stack
- Specific power: 650 W/kg for system, 2,000 W/kg for stack
- Transient response: 1 s from 10% to 90% of rated power
- Start-up time: 30 s from –20°C and 15 s from +20°C ambient temperature
- Precious metal content: 0.3 g/kW

Accomplishments

- Analyzed the performance of stacks with the 3M nanostructured thin film catalysts (NSTFC) and determined the optimum operating pressures and temperatures.
- Analyzed experimental data for Honeywell's integrated compressor-expander module (CEM) and developed a scalable compressor map, and scalable expander maps for different nozzle areas.
- Proposed and analyzed alternative CEM configurations capable of approaching the maximum parasitic power target of 5.4 kW for an 80-kW FCS.
- Analyzed the performance of advanced radiators with metal foams, high-density louver fins and microchannel plain fins. Identified a compact radiator design with the lowest pumping power.
- Analyzed the performance of enthalpy wheel humidifiers at part-load and at different rotational speeds.
- Analyzed the performance of a membrane humidifier and determined the conditions of optimum operating temperature and pressures at part-load.
- Compared the performance of two FCSs, one with an enthalpy wheel humidifier and the other with a membrane humidifier.

Introduction

While different developers are addressing improvements in individual components and subsystems in automotive fuel cell propulsion systems (i.e., cells, stacks, balance-of-plant components), we are using modeling and analysis to address issues of thermal

and water management, design-point and part-load operation, and component-, system-, and vehicle-level efficiencies and fuel economies. Such analyses are essential for effective system integration.

Approach

Two sets of models are being developed. The GCtool software is a stand-alone code with capabilities for design, off-design, steady-state, transient, and constrained optimization analyses of FCSs. A companion code, GCtool-ENG, has an alternative set of models with a built-in procedure for translation to the MATLAB/SIMULINK platform commonly used in vehicle simulation codes such as PSAT.

Results

Fuel Cell Stack Performance

In Fiscal Year 2007, we changed our reference FCS configuration (see Figure 1) to include alternative membrane electrode assemblies that use 3M nanostructured thin-film ternary Pt catalysts supported on organic whiskers [1]. In FY 2008, we received polarization curves from 3M for an optimized NSTFC electrode structure with a reduced Pt loading of 0.15 mg/cm^2 in the cathode and 0.1 mg/cm^2 in the anode [2]. We used the data to conduct a study to determine the minimum Pt content (g/kW) as a function of the stack temperature at constant 50% system efficiency at rated power. Figure 2(a) shows the calculated stack operating pressure as a function of the stack temperature. The issue of water management dictates that the operating pressure must increase as the stack temperature is raised. The NSTFC stack can be operated at ambient pressure if the stack temperature is 75°C or lower. We calculate an optimum operating pressure of 2.5 bar at 90°C stack temperature and 3 bar at 100°C stack temperature. The lower the stack temperature (and pressure) the higher is the optimum relative humidity (although the dew point temperature decreases with decrease in stack temperature) of the feed anode and cathode streams. Increasing the stack temperature (and, therefore, the pressure) incurs greater parasitic power for the air management system that must be compensated for by operating at a higher cell voltage to maintain the same system efficiency. We estimate ~30% lower Pt content if the stack is operated at 90°C and 2.5 bar rather than at 75°C and near-ambient pressure (Figure 2b). Figure 2c shows that the stack power density (based on the active membrane area) improves from 530 mW/cm^2 to 715 mW/cm^2 as the stack temperature is increased from 75°C to 90°C (and the operating pressure is raised from 1.2 bar to 2.5 bar) because of the concurrent increase in the Nernst potential and reduction in the cathode overpotential (due to faster oxygen reduction reaction kinetics). The study indicates only a marginal improvement in power density and Pt content as the stack temperature is further raised above 90°C in part because of the dilution of the reactants due to greater humidification requirements. At 90°C stack temperature, the overall Pt content is ~0.35 g/kW with 0.15 mg/cm^2 Pt in the cathode, which is about 15% lower than ~0.4 g/kW with 0.2 mg/cm^2 Pt in the cathode as in the FY 2007 reference system.

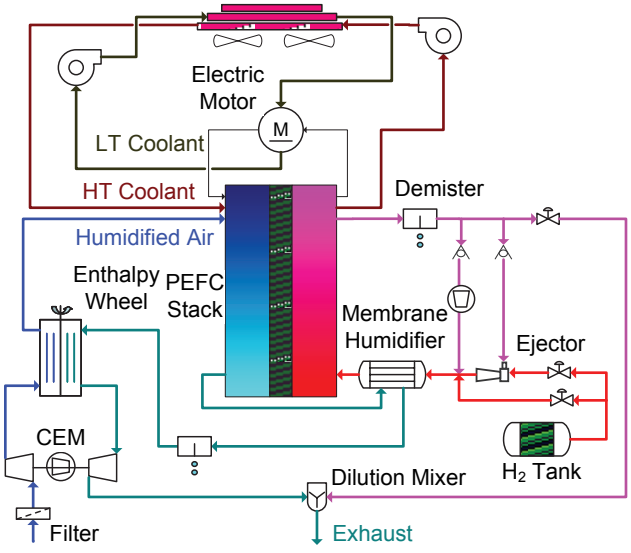

FIGURE 1. Reference Pressurized FCS with Enthalpy Wheel Humidifier

Air Management

We analyzed data from Honeywell on the performance of an integrated compressor-expander module [3] and constructed a scalable compressor map that determines the pressure ratio and efficiency as functions of the corrected shaft speed (rpm) and mass flow rate. We also constructed scalable expander

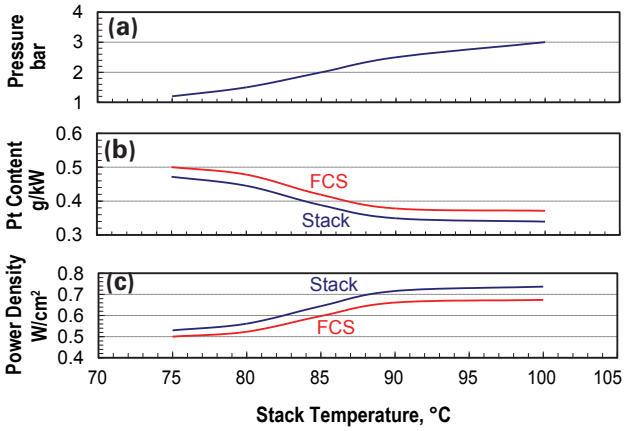

FIGURE 2. Effect of NSTFC Stack Temperature on Operating Pressure (a), Pt Content (b) and Power Density (c)

maps to determine the pressure ratio and efficiency as functions of the velocity parameter and the corrected shaft speed for different nozzle areas. The maps were used to model the performance of matched compressors and expanders on a common shaft for the 80-kW reference fuel cell system: 2.5 bar at rated power, 80°C stack temperature, 91 g/s dry air flow rate, 3 psi pressure drop between the compressor exit and turbine inlet, and 100% relative humidity at turbine inlet. The model indicated that with a fixed nozzle, the parasitic power was ~9.6 kW, which greatly exceeds the DOE target of 5.4 kW and that the compressor delivery pressure was much lower than the specifications for part- load operation.

Having identified the limitation of a fixed-area nozzle turbine in meeting the targeted pressure profile at part load, attention was focused on a variable-area nozzle turbine (VNT). We developed a method of determining the nozzle area at part-load for optimum performance and used it to determine the optimum compressor delivery pressure by matching the performance of a cathode membrane humidifier with a NSTFC stack operating at 90°C cell temperature. We concluded that with an actuator (step-up motor), the nozzle opening can be controlled to match any desired pressure vs. load profile.

We investigated different methods of cooling the CEM motor as a way of reducing the CEM parasitic power. Figure 3 compares the parasitic power for five different configurations in which the foil air bearing and rotor are cooled either by compressor suction air or by compressor discharge air, with or without a splitter (venturi, orifice or flow controller), and with an internal or an external heat exchanger. Our conclusion is that the CEM parasitic power can be reduced by 30% by redesigning the motor cooling arrangement. Further improvement in compressor and expander aerodynamics is needed to meet the DOE target of no more than 5.4 kW CEM parasitic power for an 80-kW FCS.

Thermal Management

We revisited the issue of thermal management for automotive fuel cell systems with advanced radiator designs based on metal foams and microchannel construction. Recent data from Honeywell confirms the literature values for permeability and inertial drag coefficient of commercial metal foams [4]. Our analyses showed that for a given face velocity, metal foams (40 pores per inch, 92% porosity) can have 30-45% higher effective heat transfer coefficient than the standard automotive louver fins (15 fins/inch) but also 5-15 times higher skin friction coefficient. For given frontal area and grill/under-hood designs, our model indicated that the foam radiator would be bulkier and would require much greater pumping power than the standard automotive radiator. For this reason, commercial foams are not considered good candidates for automotive radiators. We have also compared the performance of advanced automotive (louver fins, 25 fins/inch) and microchannel (plain rectangular fins, 40 fins/inch) radiators with the standard automotive radiator. Our analyses showed that compared to the standard louver fins, and depending on the face velocity, the effective heat transfer coefficient can be 40-45% higher for the advanced louver fins and 65-70% higher for the microchannel fins. Also, whereas the effective friction coefficient is 110% higher for the advanced louver fins and 220% higher for the microchannel fins at low face velocities (2 m/s), the difference in friction coefficients is quite small at high face velocities (10-15 m/s). For given frontal area and grill/under-hood designs, our model indicated that the advanced automotive radiator can be significantly more compact (70% smaller in depth) than the standard automotive radiator. Under the same conditions, the microchannel radiator can be even more compact while also requiring much lower pumping power (see Figure 4). In the coming year, we will work with Honeywell to experimentally validate our model and confirm the merits of the microchannel design over the other advanced and standard louver fin designs. Honeywell will also address the issues of manufacturability and fouling.

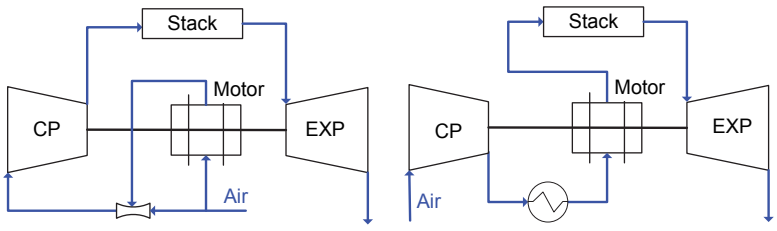

TC5: Based on Honeywell Patent US 7,056,132 B2

TC4: CEM with external heat exchanger

	Compressor		Efficiency		Power		
	Air Flow	P	CP	EXP	CP	EXP	Net
	g/s	bar	%	%	kW	kW	kWe
TC5	91	2.57	69.4	75.3	14.0	6.3	9.1
TC1	110	2.50	72.6	75.5	14.5	6.1	9.9
TC2	110	2.50	72.6	75.5	14.5	7.4	8.3
TC3	91	2.56	73.1	75.5	12.3	6.3	7.0
TC4	91	2.62	73.2	75.4	12.5	6.3	7.3

FIGURE 3. Performance of Alternative CEM Configurations (CP: compressor, EXP: expander)

Water Management

In the area of water management, we expanded our model for the enthalpy wheel humidifier (EWH) by including oxygen leakage from the cathode air due to volume exchange caused by rotation of the coated monolith. Our model showed that ~2.5% O_2 leaks across the EWH in the reference pressurized FCS at rated power (with corresponding increase in compressor power for given oxygen utilization), which increases to 10-15% at low loads if the wheel speed is held constant at 40 rpm. We also conducted a parallel study to assess the need to pre-cool (or pre-heat at part-load) the compressor discharge (the temperature can exceed 160°C if ambient air at 40°C is compressed to 2.5 bar) if the EWH is substituted with a membrane humidifier (MH). We found that there exists an optimum temperature (~70°C for the reference FCS with NSTFC stack at 90°C) at which the rate of water-vapor mass transfer between the dry compressed air and saturated spent cathode air is highest. The membrane area has to increase by ~50% if the dry air temperature is 85°C (too hot) and by ~100% if the temperature is 40°C (too cold).

We conducted a study to determine the impact of the humidification device (EWH or MH) on the performance of the reference FCS. The main results from the study are summarized below.

- Whereas the spent cathode air is heated in the EWH at the rated power point, it is cooled in the MH because of the presence of the precooler. Consequently, the expander recovers more power in the FCS with an EWH and the CEM parasitic power is lower.
- The heat transferred in the MH precooler (~8.1 kW) is of low grade, it must be absorbed by the coolant in the low-temperature circuit, and it is difficult to reject.

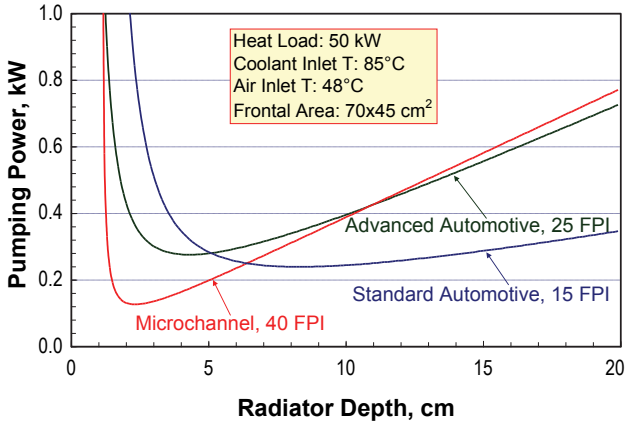

FIGURE 4. Relative Performance of Advanced Automotive Radiator Designs (FPI: fins per inch)

- At constant wheel speed, the dew point temperature of the cathode air leaving the EWH increases as the air flow rate is reduced (part-load operation) because of the combined effects of the lower compressor discharge temperature and the greater residence time.
- With a precooler upstream of the MH, the dew point temperature of the cathode air decreases at part-load because of the lower compressor discharge pressure.
- The FCS with MH needs to operate at higher pressures at part-load and attains lower efficiency than the system with EWH (for systems with same cell voltage at rated power).

Conclusions and Future Directions

- It appears possible to achieve an overall Pt content of 0.35 g/kW (for a system with 50% efficiency at 2.5 bar, 90°C cell temperature) by using an optimized NSTFC electrode structure with 0.25 mg/cm^2 total Pt loading in cathode and anode ternary electrocatalysts.
- Compared to operation at 75°C and near-ambient pressure, the overall Pt content can be reduced by ~30% if the NSTFC stack is operated at 90°C and 2.5 bar pressure. Further increases in stack temperature introduce only marginal reduction in Pt requirement.
- A CEM based on the Honeywell design (mixed axial flow compressor, radial inflow turbine) can meet the DOE pressure specifications at part-load by controlling the nozzle area. It appears possible to reach the optimum operating pressures at part-load by using the VNT.
- The CEM parasitic power can be reduced by ~30% by employing alternative methods of cooling the air foil bearing and rotor. Further improvements in aerodynamics are needed to reach the DOE target of no more than 5.4 kW parasitic power (for 91 g/s air flow rate, 2.5 bar discharge pressure).
- Advanced radiators using high density louver fins or plain rectangular fins can be more compact and require less pumping power than the standard automotive designs.
- The reference FCS with an EWH shows better performance (efficiency and heat rejection) than a system with a MH.
- In FY 2009, we will include the aspects of stack start-up and shut-down that affect system design and performance. We will validate our models for the thermal management and water management components with the experimental data to be taken at Honeywell. We will also conduct studies on the dynamic performance of the FCS under real-world driving conditions.

FY 2008 Publications/Presentations

1. R. K. Ahluwalia and X. Wang, "Effect of CO and CO_2 Impurities on Performance of Direct Hydrogen Polymer-Electrolyte Fuel Cells," *J. Power Sources*, 180 (2008), 122.

2. R. K. Ahluwalia and X. Wang, "Fuel Cell Systems for Transportation: Status and Trends," *J. Power Sources*, 177 (2008), 167.

3. R. K. Ahluwalia and X. Wang, "Buildup of Nitrogen in Direct Hydrogen Polymer-Electrolyte Fuel Cell Stacks," *J. Power Sources*, 17 (2007), 63.

4. R. K. Ahluwalia, X. Wang, S. Lasher, J. Sinha, Y. Yang, and S. Sriramulu, "Performance of Automotive Fuel Cell Systems with Nanostructured Thin Film Catalysts," *2007 Fuel Cell Seminar & Exposition*, San Antonio, Oct. 15–19, 2007.

5. R. K. Ahluwalia, X. Wang and R. Kumar, "Fuel Cell Systems for Transportation: Status and Trends," *EET-2007 European Ele-Drive Conference*, Brussels, Belgium, May 30 – June 01, 2007.

6. R. K. Ahluwalia and X. Wang, "Approach for Validating Model for CO Poisoning of PEFC Anodes," *North American Fuel Hydrogen Quality Team*, PG&E Headquarters, San Francisco, Apr. 1–2, 2008.

7. R. K. Ahluwalia and X. Wang, "Effect of Fuel Impurities on Performance of Fuel Cells: Model Development," *10th Meeting of ISO/TC 197/WG 12*, Montecatini Terme, Italy, Nov. 6–7, 2007.

8. R. K. Ahluwalia and X. Wang, "Modeling for Hydrogen Quality: Effect of Fuel Impurities on Performance of Fuel Cells," *Hydrogen Quality Modeling Workshop*, ANL, Argonne, IL, Aug. 30–31, 2007.

9. R. K. Ahluwalia, X. Wang, R. Kumar, S. Lasher, J. Sinha, Y. Yang and S. Sriramulu, "Performance of Automotive Fuel Cell Systems for Light Duty Vehicles," *IEA Annex XX Meeting*, Petten, The Netherlands, May 28-29, 2007.

References

1. R. K. Ahluwalia, X. Wang, S. Lasher, J. Sinha, Y. Yang, and S. Sriramulu, "Performance of Automotive Fuel Cell Systems with Nanostructured Thin Film Catalysts," *2007 Fuel Cell Seminar & Exposition*, San Antonio, Oct. 15-19, 2007.

2. M. K. Debe and A. J. Steinbach, Personal communications, 2008.

3. M. Gee, Personal communications, 2008.

4. Z. I. Mirza and V. Patel, Personal communications, 2008.